Experimental Cell Research 386 (2020) 111684

Contents lists available at ScienceDirect

Experimental Cell Research

journal homepage: www.elsevier.com/locate/yexcr

Establishment of a novel cancer cell line derived from vulvar carcinoma associated with lichen sclerosus exhibiting a fibroblast-dependent tumorigenic potential

Harsh Dongre[a,b], Neha Rana[a], Siren Fromreide[a], Saroj Rajthala[a,b], Ingeborg Bøe Engelsen[c], Justine Paradis[d], J. Silvio Gutkind[d,e], Olav Karsten Vintermyr[a,f], Anne Christine Johannessen[a,b,f], Line Bjørge[b,c], Daniela Elena Costea[a,b,f,*]

[a] The Gade Laboratory for Pathology, Department of Clinical Medicine, Faculty of Medicine, University of Bergen, Norway
[b] Centre for Cancer Biomarkers (CCBIO), Faculty of Medicine, University of Bergen, Bergen, Norway
[c] Department of Obstetrics and Gynecology, Haukeland University Hospital, Bergen, Norway
[d] Moores Cancer Center, University of California, San Diego, La Jolla, CA, USA
[e] Department of Pharmacology, University of California, San Diego, La Jolla, CA, USA
[f] Department of Pathology, Haukeland University Hospital, Bergen, Norway

ARTICLE INFO

Keywords:
Vulvar lichen sclerosus
Vulva squamous cell carcinoma
Novel cell line
3D organotypic models
In vivo tumorigenicity

ABSTRACT

Vulvar squamous cell carcinoma associated with lichen sclerosus (VLS-VSCC) are rare tumors but with higher recurrence and worse prognosis than other types of VSCC. Lack of experimental models has limited the search for better understanding of the biology and development of treatment modalities. In this study, we isolated and characterized primary cells from VSCC (n = 7) and normal vulvar tissue adjacent to tumor (n = 7). Detailed characterization of the novel spontaneously immortalized cell line, VCC1 revealed a characteristic epithelial morphology *in vitro* and a well-differentiated keratinizing SCC histology *in vivo*, closely resembling the tumor of origin. VCC1 expressed higher levels of epithelial-mesenchymal transition markers and higher clonogenic properties as compared to other established non VLS-VSCC cell lines. *In vitro* 3D organotypic assays and *in vivo* xenografts revealed a prominent role of cancer-associated fibroblasts in VCC1 invasion and tumor formation. In conclusion, VCC1 mirrored several major VLS-VSCC features and provided a robust experimental tool for further elucidation of VLS-related oncogenesis and drug testing.

1. Introduction

With an incidence of 0.5–1.5 in 100,000 individuals per year, carcinoma of the vulva represents about 4% of all female genital cancers [1]. Of these, nearly 90% of cases are squamous cell carcinomas (VSCC). It is well documented that VSCC develops from premalignant vulvar intraepithelial neoplasia (VIN) lesions [2,3]. Previously, VIN was graded into three subtypes: VIN 1 (mild dysplasia), VIN 2 (moderate dysplasia) and VIN 3 (severe dysplasia). However, clinico-pathological data did not support the presence of such continuum [4]. According to the latest and widely accepted grading system, the previously used VIN terminology has been replaced by cytology-based squamous intraepithelial lesions (SIL) terminology [5,6]. Consequently, these precancerous lesions are divided into three types: low-grade squamous intraepithelial lesions (LSIL, VIN1); high-grade intraepithelial lesions (HSIL, VIN 2,3 or usual VIN) and a very differentiated variant, called dVIN. Such grading systems correlates with the risk to cancer progression over time [6].

In addition, mounting evidence suggests that there are two different pathological pathways governing the development of VSCC: human papillomavirus (HPV) -independent and HPV-dependent [6]. HPV-dependent VSCC show a more profound cellular atypia and are histologically warty/basaloid [6]. These are more common in younger women and have HSIL as their precursors [6]. On the other hand, HPV-independent VSCC show basal atypia and often presents a more keratinized histology [6,7]. These typically occur in elderly women, develop on dVIN background and have a high malignant potential [8]. Moreover, these are often associated with inflammatory conditions such as vulvar lichen sclerosus (VLS) [3], a chronic inflammatory dermatitis [9]. Histologically, VLS exhibits a thinned epithelium with hyper-

* Corresponding author. Department of Clinical Medicine, Faculty of Medicine, University of Bergen, 5009 Bergen, Norway.
E-mail address: Daniela.Costea@uib.no (D.E. Costea).

https://doi.org/10.1016/j.yexcr.2019.111684
Received 20 May 2019; Received in revised form 15 October 2019; Accepted 19 October 2019
Available online 23 October 2019

keratinization, a band of hyalinized collagen lacking vessels and a lymphocytic infiltrate beneath [10]. An association between VLS and VSCC is well-documented [3]. Although the risk for these lesions to progress to VSCC is low (3–7%) [3,11], approximately 30–60% of vulvar SCC occur on a VLS background that often is undiagnosed due to lack of serious clinical symptoms [3,10,12].

There is a dearth of knowledge about the key molecular events involved in vulva cancer in general and VLS-VSCC in particular, which can be used as predictive markers or as therapeutic targets. In addition, the role of stromal component of the tumor microenvironment (TME), especially carcinoma-associated fibroblasts (CAFs) in VLS-VSCC is unknown. This is due to the lack of well-established experimental models. Better understanding of this cancer is required at the genetic, molecular, and cellular level. The aim of this study was to establish and characterize robust experimental models for studying VLS-VSCC. To the best of our knowledge, this is the first successful attempt to establish a cell line from VLS-VSCC. We describe here 3D collagen co-culture models for studying tumor-stroma crosstalk and *in vivo* xenografts in immunodeficient mice using this cancer cell line and vulvar CAFs. This study provides a thorough *in vitro* and *in vivo* characterization and validation of a human-tissue based biological tool relevant for further studies on VLS-VSCC.

2. Materials and methods

2.1. Sample collection and patient history

Human VSCC tissues (n = 7) along with their respective non-cancer adjacent tissues (normal epithelial tissue, 1 cm away from the tumor margin showing no histological signs of atypia) were collected from patients undergoing surgical resection at the Department of Obstetrics and Gynecology, Haukeland University Hospital, Bergen, Norway. Written informed consent was obtained from all patients and the Regional (REK Vest, Norway) Committee for Medical and Health Research Ethics (REK nr. 2017/279) approved the study. The samples were included in Bergen Gynecologic Cancer Biobank, Bergen, Norway (REK nr. 2014/1907). Isolation of vulva cancer cells (VCC) and matched vulva cancer-associated fibroblasts (VCAF) was successful in 57% (n = 4/7) and 100% (n = 7/7) cases, respectively. Besides, normal vulvar keratinocytes (NVK, n = 5/7, 71%) and normal vulvar fibroblasts (NVF, n = 7/7, 100%) from normal adjacent tissue were also isolated successfully. Out of the four primary cancer cell lines isolated, only one could be propagated indefinitely without implementing additional genetic alterations. This cell line, VCC1 was established from a VSCC of an 84-year old woman who presented with a 4 cm tumor in size. Histopathological examination of the whole specimen, including surrounding tissue was compatible with a HPV negative, VLS associated keratinizing type VSCC, FIGO stage 1B. The patient is still alive without recurrence 22 months after the primary surgery.

2.2. Isolation of normal primary keratinocytes and fibroblasts

Primary keratinocytes and fibroblasts were isolated from apparent normal adjacent tissue to tumor by enzyme digestion. These tissue samples were incubated in 2.5 mg/ml dispase (GIBCO, Paisley, UK) overnight at 4 °C. The following day, epithelium was detached from the underlying stroma, minced into small pieces, and treated with 0.5% trypsin (GIBCO, Paisley, UK) for 5 min at 37 °C. Further, the pieces were neutralized with New-Born Calf Serum (NBCS, GIBCO, Auckland, NZ), and mechanically dissociated using Pasteur pipettes. The single cell suspension thus formed was plated in a 6-well plate (Sarstedt, Nümbrecht, DE) in keratinocyte serum-free medium (KSFM, GIBCO, Paisley, UK) in a humidifying chamber in 5% CO_2 at 37 °C (standard culture conditions). Similarly, for the fibroblast isolation, the underlying stroma left after detachment of the epithelium was cut into smaller pieces and treated with 1 mg/ml collagenase (GIBCO, Paisley, UK) for 30 min at 37 °C. Following neutralization with NBCS, the cells were cultured in Dulbecco's Modified Eagle's medium (DMEM, Sigma-Aldrich, St. Louis, US) supplemented with 10% NBCS (DMEM complete) under standard culture conditions. Adherents cells were first observed after four days, and keratinocytes-like and fibroblasts-like cell lines were sub-cultured after nine days in their respective media.

2.3. Isolation of VCC and VCAF from tumor tissue by explant culture method

The tumor tissue was cut in small pieces (1–2 mm^2) and allowed to adhere on several culture plates. After attachment, the plates were flooded with DMEM complete medium and cultured further. Initial outgrowth of both VCC and matched VCAF was observed after four days. The plates containing majority of explants with epithelial-like cell outgrowth were marked as VCC and explants with outgrowth of fibroblast-like morphology were scrapped-off and vice versa for VCAFs. Further, to clean the cancer cells of fibroblast-like cells and vice-versa, selective trypsinization (3min for VCAF and 7min for VCC) was done on 9th day. This was followed by serial dilution of VCC in 48 well-plate (Sarstedt, Nümbrecht, DE). After 4–6 days, the morphology of growing cells was assessed and wells with only epithelial-like morphology were selected for further propagation. In case of VCC1, only 6 wells out of 48 had pure epithelial-like morphology. These were mixed and cultured together to avoid selecting single clonal population. The growth media used was FAD [13]. For VCAF, 3min trypsinized cells were sub-cultured in DMEM complete. UMSCV1A and UMSCV4, well-established vulva cancer cell from non-VLS patients were purchased from Thomas Carey, University of Michigan, US for comparative studies [14]. All cell lines were routinely checked for mycoplasma contamination by using MycoAlert mycoplasma kit (LONZA, Rockland, US) and tested negative.

2.4. Flow cytometry

Expression of lineage-specific markers was assessed by flow cytometry (BD Accuri C6 cytometer, Ann Arbor, US). Cells were trypsinized and stained with antibodies listed in Table S1. Isotype control mouse IgG_1-APC and IgG_1-PE were used for normalization. 30,000 cells were collected for analysis and cell debris were excluded by gating. Expression of each antigen was analyzed by FlowJo v10 software (FlowJo LLC, Ashland, US).

2.5. Growth kinetics and cell cycle analysis

The population doubling time (PDT) was determined by cell viability assay based on trypan blue dye exclusion principle. Number of cells was counted every 24hr in an automated counting chamber (TC20-Biorad, Hercules, US). The doubling time was calculated using standard formula mentioned elsewhere [15]. For cell cycle analysis, VCC1 were grown in serum-deprived medium for 48hr and then harvested at regular intervals up to 30hr. For harvesting, cells were trypsinized, washed with PBS, fixed in 2 mL ice-cold 70% ethanol and stained for 30 min at room temperature (RT) in dark with 0.025 mg/mL propidium iodide (PI), 0.1% Triton X-100 and 0.05 mg/mL ribonuclease A (all from Sigma-Aldrich, St. Louis, US) in PBS. Total PI content was determined by Accuri C6 flow-cytometer and cell cycle distribution was quantitated by ModFit LT software (Verity, Maine, US).

2.6. DNA extraction and short tandem repeats (STR) profiling

Ten-micron thick sections were cut from formalin fixed paraffin embedded (FFPE) tissue block of the original tumor. Genomic DNA (gDNA) was extracted from the tumor tissue and cell lines (VCC1 and VCAF1) using Nucleopsin DNA FFPE kit (Macherey-Nagel GmbH, Germany) and E.Z.N.A FFPE DNA kit (Omega Bio-Tek Inc., Norcross, US) respectively, according to manufacturer's protocol. Further,

AmpFlSTR® Profiler Plus amplification kit (Applied biosystems [AB], Carlsbad, US) was used to detect nine tetranucleotide STR loci and the Amelogenin gender-determining marker in a single PCR amplification tube (Table S2). Amplification by polymerase chain reaction (PCR) was carried out in AB 2720 Thermal cycler (AB, Carlsbad, US). After PCR amplification, the products were separated and analyzed using capillary electrophoresis on an ABI 3500XL genetic analyzer (AB, Carlsbad, US).

2.7. Colony and sphere formation assays

Colony and sphere formation assays were performed following a protocol mentioned elsewhere [16]. Three independent experiments were performed for each cell line. Representative images for both assays were acquired on DM IRB inverted microscope (Leica, Houston, US).

2.8. Hr-HPV DNA and gene expression analysis

Total RNA was extracted from cells using RNeasy Mini kit (Qiagen, Oslo, NO). Following manufacturer's protocol, 300 ng of total RNA was converted to cDNA using High-Capacity cDNA Kit system (AB, Carlsbad, US). For tumor tissue, gDNA isolated previously from the tumor FFPE block was used. Hr-HPV16 E6/E7 DNA was detected using quantitative reverse transcription PCR (RT-qPCR) following manufacturer's protocol using SYBR green primers (Table S3). Absence of non-specific amplifications was confirmed by running the PCR products on agarose gel with ethidium bromide. UMSCV6, a known HPV16 E6/E7 positive cell line was used as positive control [14]. For gene expression analysis, all RT-qPCR amplifications were performed for 40 cycles using AB 7500 PCR system (AB, Carlsbad, US) for TaqMan probes mentioned in Table S3. The expression levels of all genes were normalized to GAPDH and the fold changes generated by $2^{-\Delta\Delta Ct}$ method were plotted as heatmap.

2.9. 3D organotypic co-culture (3D OTC) models

3D OTC were engineered by growing cancer cells on top of collagen type I (Corning, Bedford, US) matrix populated with and without fibroblasts using a protocol well-established in our laboratory [13]. These were cultured in serum-free DMEM with 50 μg/ml L-ascorbic acid, 0.4 μg/ml hydrocortisone, 5 μg/ml insulin, 20 μg/ml transferrin and 7.5% bovine serum albumin (all from Sigma, St. Louis, US) for 3 days. On the 4th day, the cultures were lifted at air–liquid interface and cultured further for 9 days in the same medium. On 13th day, they were harvested, fixed in formalin and embedded in paraffin for histological and immunohistochemical staining.

2.10. Immunohistochemistry and immunofluorescence

Immunohistochemical staining was performed using EnVision + Detection Systems, Peroxidase/DAB, Rabbit/Mouse (Agilent Dako, Golstrup, DK) according to standard protocol [17]. Details of primary antibody dilution and epitope retrieval buffers used are listed in Table S1. Images were acquired using a whole slide scanner (Hamamatsu NanoZoomer-XR, Japan).

For immunofluorescence, cells grown on coverslips were fixed with 4% paraformaldehyde for 15min and incubated with primary antibodies (Table S1) for 1 h at RT. Following PBS washes, cells were incubated with Alexa Fluor 488 anti-mouse secondary antibody for 1 h at RT, counterstained with 4', 6-diamidino- 2-phenylindole (DAPI, Sigma-Aldrich, Oslo, NO), mounted and viewed under a fluorescence microscope (Axio Imager Z2, Carl Zeiss, DE).

2.11. Quantification of depth of invasion and number of invading cells

Depth of invasion and number of invading VCC1 was measured on anti pan-cytokeratin immunostained tissue sections using a standard protocol mentioned elsewhere [18]. For the measurement, 3D OTC constructed with (NVF1 and VCAF1) and without fibroblasts were used.

2.12. In vivo tumorigenic assay

Four to five week old thirty-six NOD/SCID IIγ2R deficient female mice were obtained from Jackson Laboratories (Bar Harbor, ME, US) [19]. The mice were divided randomly in two groups with one group receiving cells resuspended in PBS in a total injection volume of 100 μL alone (n = 18) or in a 1:1 mixture of PBS and matrigel (n = 18). Further, these groups were subdivided equally, and the mice were injected subcutaneously with logarithmically growing 1×10^6 VCC1, alone (n = 9) or with 1×10^5 VCAF1 (ratio 1:10, n = 9). Animals were examined twice per week for 7 weeks for the development of tumors. Tumor volume was calculated as: volume, V (in mm^3) = $(LXW^2)/2$, where L is tumor length and W is tumor width. Mice with tumors were sacrificed after 7 weeks. The excised tumors were fixed in 10% formalin and further processed for histopathology. This study was approved by the ethical board (S15195) and carried out at the Animal Research Facility at University of California, San Diego, US.

3. Results

3.1. A novel VLS-VSCC cell line

A cell line was successfully established *in vitro* from a surgically resected primary VLS-VSCC tumor. The established cell line has been successfully frozen, resuscitated and cultured in FAD medium for more than 21 months (220 PDs). In monolayer culture, VCC1 grew mainly in tight clusters of polygonal cells as adherent colonies with epithelial morphology (Fig. 1A a-d). The isolated matched VCAF1, displayed a characteristically fibroblast-like, spindle-shaped morphology and grew as loose cells (Fig. 1A e-h). Immunofluorescent staining of VCC1 showed cytokeratin 10 (CK10) staining and weak vimentin staining (Fig. 1Ba, b). In contrast, VCAF1 were negative for CK10 and positive for vimentin (Fig. 1B c, d). In addition to this, VCC1 expressed pan-cytokeratin (AE1/3), CK8, CK18, and stem cell markers such as ALDH1, CD44 and Oct 3/4 (Fig. S1 A).

As indicated by flow cytometry, majority of VCC1 expressed epithelial cell-adhesion molecule, EpCAM; however, a subpopulation (< 2%) of cells expressed both EpCAM and mesenchymal lineage specific cell surface antigen, beta-type platelet-derived growth factor receptor (PDGFR-β, CD140b). Moreover, the cells also expressed CD146 (~6%), a marker of pericytes and mesenchymal stem cells [20]. Contrary to this, majority of VCAF1 expressed CD140b but not EpCAM or CD146 (Fig. 1C). Neither VCC1 nor VCAF1 (< 1%) expressed CD31, an endothelial cell marker (Fig. 1C).

3.2. STR profiling validates authenticity of VCC1

In order to rule out cross-contamination with other cell lines and to confirm the authenticity of isolated cell lines, VCC1 and VCAF1 were subjected to STR DNA profiling against the original tumor tissue. Out of 9 markers and Amelogenin gender-determining marker tested, both the VCC1 and VCAF1 expressed all but one marker (≥80% match, meeting the acceptance criteria) confirming authenticity of the cell lines (Table S2).

3.3. VCC1 is more clonogenic than non VLS-VSCC cell lines

The colony-forming ability of VCC1 was compared against NVK and VSCC cell lines from non-VLS patients, UMSCV1A and UMSCV4. UMSCV1A is known to exhibit a biologically aggressive behavior *in vivo,* whereas UMSCV4 displays a more passive behavior [14,21]. VCC1 formed significantly more colonies *in vitro* than UMSCV1A and UMSCV4, suggesting a higher clonogenic and proliferative potential

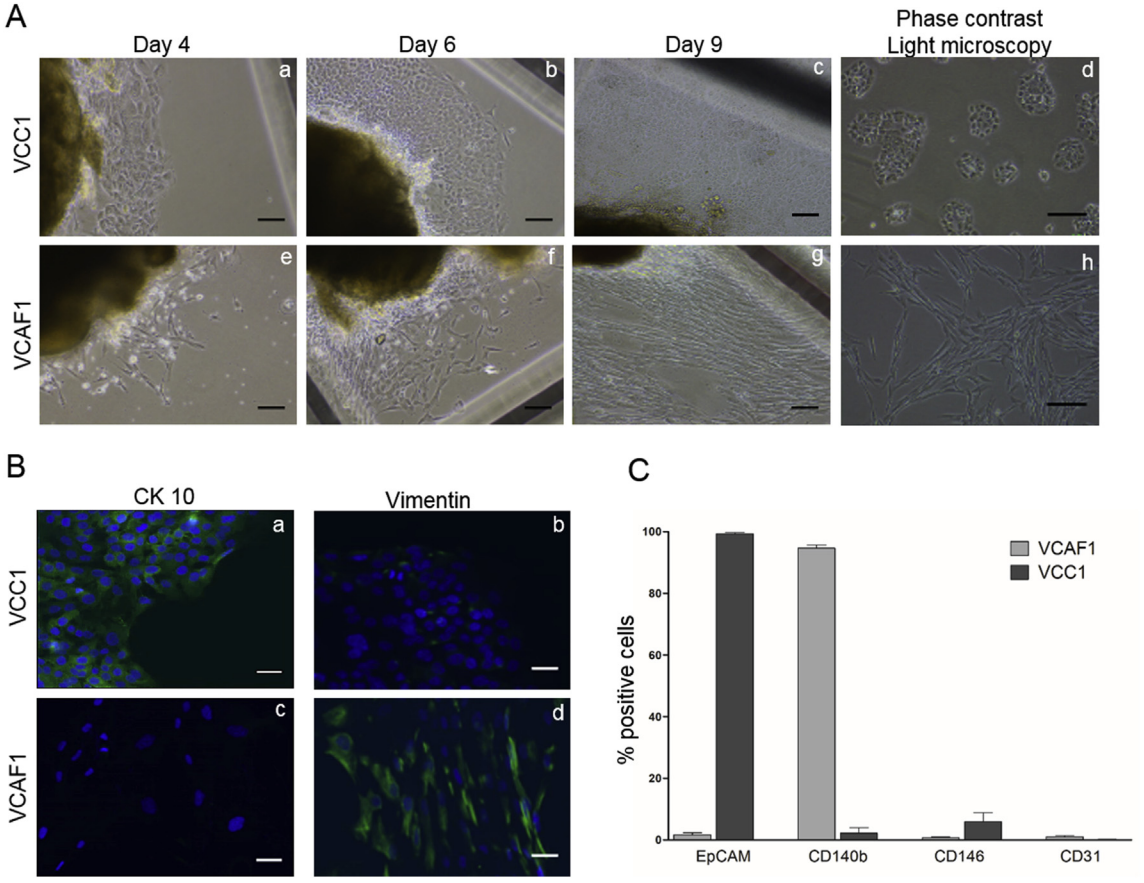

Fig. 1. Isolation and characterization of vulva cancer cells (VCC1) and vulva cancer-associated fibroblasts (VCAF1). A) Representative phase contrast images showing outgrowth of cancer cells and fibroblasts at day 4 (a, e), day 6 (b, f) and day 9 (c, g) respectively. Morphology of VCC1 is mainly polygonal (d) whereas VCAF1 were more spindle-shaped and formed loose cell aggregates (h). Scale bar- 50 μm. B) Immunofluorescence staining showed cytokeratin 10 (CK10, green, a) positive cancer cells and sparsely positive cells for vimentin (green, b). In case of fibroblasts, no staining for CK10 was detected whereas it was positive for vimentin (green, c and d). Nuclei are counterstained with DAPI (blue). Scale bar- 100 μm. C) Comparison of expression of EpCAM, CD140b, CD146 and CD31 in between VCAF1 and VCC1 using flow cytometry. Flow cytometry results are expressed as mean ± SD of three independent experiments. (For interpretation of the references to colour in this figure legend, the reader is referred to the Web version of this article.)

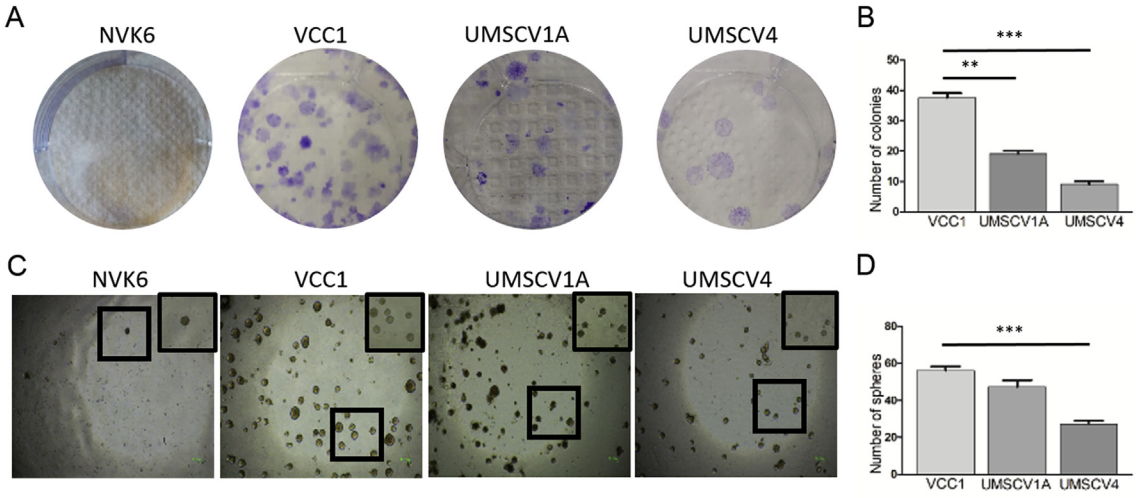

Fig. 2. VCC1 is more clonogenic in comparison to UMSCV1A and UMSCV4. A) Representative micrographs of adherent colonies from NVK6, VCC1, UMSCV1A and UMSCV4. B) Quantification of adherent colony-formation assay. The number of colonies was counted manually after staining with crystal violet. VCC1 formed statistically more number of colonies than UMSCV1A and UMSCV4. C) Representative images of formed tumor-spheres. D) Quantification of the sphere formation assay. The spheres were counted using a stereo microscope at X100 magnification. VCC1 formed more number of spheres than UMSCV1A and UMSCV4. Note that NVK did not form colonies or spheres and thereby they were excluded from the statistical analysis. Experimental data is expressed as mean ± SD of three independent experiments and analyzed using Students t-test. **$p < 0.01$ and ***$p = 000.1$. (For interpretation of the references to colour in this figure legend, the reader is referred to the Web version of this article.)

(Fig. 2 A, B). Also, VCC1 formed statistically significant more spheres than UMSCV4 and comparable to but bigger in size than UMSCV1A (Fig. 2 C, D).

3.4. Growth characteristics of VCC1 in vitro and in vivo

PDT of VCC1 at different passages revealed an average doubling time of 18.90 ± 0.53hr. This was however less than that of UMSCV1A (30.12 ± 0.43hr) and UMSCV4 (54.7 ± 5.27hr) (Fig. S1 B). Flow cytometry analysis of PI stained VCC1 illustrated cell cycle distribution in different stages at different time points (Fig. S1 C). *In vivo* tumorigenicity showed no tumor formation in mice group receiving cells in PBS only. Interestingly, tumor formation was observed after 4 days of injection of VCC1 in combination with VCAF1 resuspended in matrigel (9/9, take rate 100%). The tumor growth was rapid for the first ten days followed by a decrease in tumor volume afterwards. For VCC1 alone in matrigel, the take rate was 33% (2/6) and the tumors were small in size (Fig. S2 A).

3.5. Genetic make-up of VCC1 reveals non-association with hr-HPV16 and an aggressive phenotype

Presence of hr-HPV16 was determined by assessing the level of transcript of HPV16 E6 and E7 and expression of protein $p16^{INK4a}$, a surrogate marker for HPV [22]. Neither patient tumor nor VCC1 derived from the tumor, expressed hr-HPV16 E6/E7 or $p16^{INK4A}$ (Fig. 3A and B). Further, expression of several carcinogenesis-related genes was profiled and illustrated here in the form of a heat map (Fig. 3C). VCC1 overexpressed *VIM* (two-folds), *TWIST1* (three-folds) and expressed *CDH1* (five-folds) at a lower level when compared to NVK thus pointing towards a more epithelial-mesenchymal transition (EMT)-like phenotype. In addition to this, several tyrosine kinases were overexpressed in VCC1 (*FGF2*- four folds, *PTK2*- two folds and *PDGFRβ*-five folds). The expression of cell cycle related genes was similar to NVK except for *CCND2* (decreased by five-folds). Of note, *ITGA11*, a gene encoding a stromal cell-surface receptor for fibrillary collagens, was overexpressed by three-folds in VCC1. In comparison, gene expression analysis of UMSCV1A indicated a more angiogenic potential but less motile genotype. UMSCV4 cells showed very few alterations except for lower expression of *VEGFA* and *VEGFC* in comparison to NVK (Fig. 3C).

3.6. Engineered VCC1 3D models show invasive potential only in presence of fibroblasts

In order to mimic the effect of fibroblasts on growth and differentiation of cancer cells, we engineered 3D OTC. VCC1 showed little to no invasion into the matrix in absence of fibroblasts (Fig. 4A b). However, cancer cells invaded the matrix in presence of both NVF1 and VCAF1 in the collagen matrix (Fig. 4A c, d). Histomorphometrical analysis revealed no significant difference in the depth of invasion between NVF1 and VCAF1. Although VCAFs supported an increased invasion (depth) of VCC1, the number of cancer cells invading into the matrix was higher in NVF1 (Fig. S3). Histologically, the architecture and the invasion pattern of engineered 3D OTC closely resembled that of the native tumor tissue from which the cell line was derived (Fig. 4A a). Immunohistochemistry revealed similar protein expression profile of pan-cytokeratin (Fig. 4B a–d), vimentin (Fig. 4B e, g, h) and E-cadherin (Fig. 4B i–l) across all 3D OTC. The protein expression for the marker of proliferation, Ki-67 (Fig. 4B m, o, p) and of differentiation, involucrin (Fig. 4B q, s, t) was similar when native tumor tissue and 3D OTC grown with fibroblasts were compared. However, 3D OTC grown without fibroblasts displayed a thicker epithelium with higher degree of differentiation but almost no proliferation (Fig. 4B r, n).

3.7. VCAF1 promotes invasive and tumorigenic potential of VCC1 in vivo

A take rate of 100% and an increase in tumor volume when compared to VCC1 alone suggests that VCAF1 promoted tumorigenic potential of VCC1 in mice xenografts. The histology of tumors formed after injection of VCC1 alone was of SCC in nature but with no invasive tumor fronts and with several cyst-like spaces (Fig. S2 B). In contrast, the tumors formed after injection of VCC1 together with VCAF1 had similar histology to the original tumor, both being well-differentiated SCC (Fig. 5A a, b). Both the original tumor and VCC1-VCAF1 xenografts had characteristic keratin pearl formation (Fig. 5B a, e) and invasive single cell islands (Fig. 5B b, f). In addition, the xenografts showed local muscular and perineural invasion similar to that observed in the original patient tumor (Fig. 5B c, d, g, h).

4. Discussion

Infrequent incidence of vulva squamous cell carcinoma associated with lichen sclerosus et atrophicus compared to other female genital cancers coupled with advanced age of patients has hampered genetic and molecular studies on VLS-related tumorigenic pathways [23,24]. This has led to minimal improvement in treatment modalities in recent decades [25]. With an estimated risk of 3–7% transformation of VLS to VSCC, this inflammatory condition demands more preclinical models to study the events in oncogenesis [11,26]. Cancer studies rely on the use of cancer cell lines [27,28], xenografts [29,30], genetically modified mice [30,31] and paraffin-embedded samples [32,33] as experimental model systems. *In vitro* tumor cell lines represent valuable tools for functional and mechanistic studies on cell processes involved in carcinogenesis [34], and a detailed characterization is fundamental before application.

A thorough literature search identified nineteen cell lines derived from squamous cell carcinoma of vulva [14,21,35,36]. Eleven of these nineteen cell lines are derived from metastatic tumors, thus leaving eight cell lines derived from primary, previously untreated tumors [21,35,36]. Remarkably, none of the cell lines are derived from VLS-VSCC, however this could be attributed to misdiagnosis and/or under reporting [10,12]. Nonetheless, even in this context, the VCC1 cell line isolated, established and characterized here, represents a novel and unique model system to study VLS-VSCC. Confirmation that the cell line was derived from corresponding tumor of the patient was provided by STR DNA fingerprinting, which demonstrated 90% identical repeats. The fact that they did not present a 100% match reflects the genomic imbalances in the tumor and/or cell line. The present characterization of VCC1 provides a make-up relevant for further studies on VLS-related tumorigenesis. Not only did these cells show capacity to expand *ex vivo* for more than 220 population doublings, they also showed (i) distinctive epithelial morphology with stem cell-like characteristics, (ii) non-association with hr-HPV16 DNA, (iii) intermediate EMT phenotype, (iv) fibroblast dependent invasion in 3D OTC, and (v) *in vivo* tumorigenesis.

Unlimited proliferation and ability to self-renew confer 'stemness' to cancer cells [37]. In this regard, we used colony and sphere formation assay to evaluate stemness. VCC1 formed statistically more colonies than well-established non VLS-VSCC cell lines reflective of enhanced capacity for proliferation. In addition, VCC1 formed more spheres than UMSCV4 but comparable to UMSCV1A. Besides to the number of spheres formed, the size of the spheres could also be indicative of higher tumorigenic potential. In the case of VCC1, both the size and number of spheres was greater than UMSCV1A and UMSCV4. Another point of interest is that VCC1 showed *in vitro* a predominantly holoclone appearance, indicating an epithelial stem-cell phenotype [38].

In most solid tumors, EMT occurs at the invasive front imparting migratory and invasive phenotype to the tumor cells. An important characteristic of EMT is loss of epithelial markers (E-cadherin and keratins), and upregulation of mesenchymal markers (vimentin, *N*-

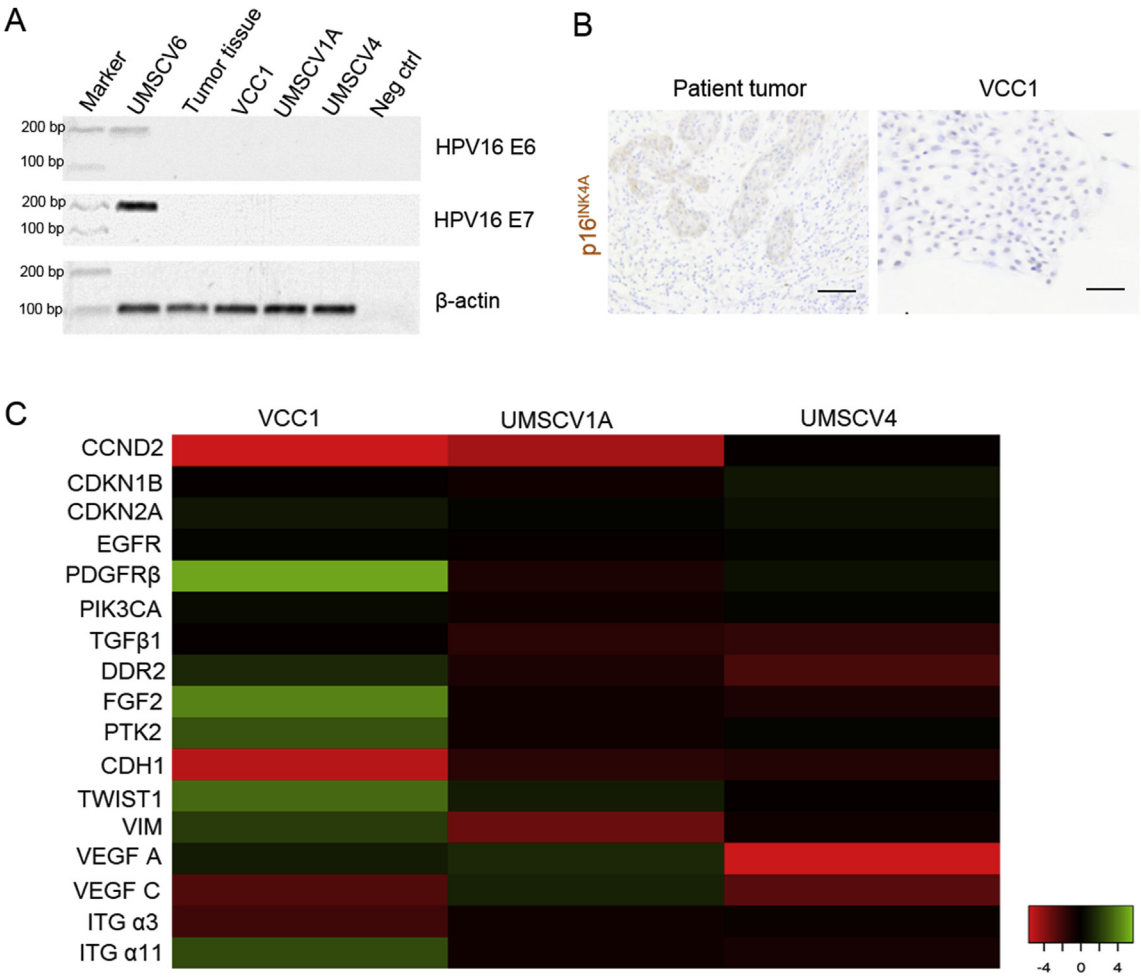

Fig. 3. Detection of hr-HPV16 DNA and heatmap of genes involved in various oncogenic processes. A) Presence of hr-HPV16 E6 and E7 gene transcript was tested in native tumor tissue, VCC1 and other VSCC cell lines using RT-qPCR. The PCR products were run on 1.5% agarose gel stained with ethidium bromide. UMSCV6 was used as positive control. B) Immunohistochemistry of native patient tumor and VCC1 for $p16^{INK4A}$ was negative. Scale bar 100 μm. C) Heatmap of gene expression in cancer cell lines. The names of cancer cell lines are listed on the top whereas the names of genes that were profiled are listed on the left of figure. A median expression value was designated as black; red as decreased expression and green as increased expression compared to NVK. Results presented here were performed in triplicate with each experiment performed further in duplicate. (For interpretation of the references to colour in this figure legend, the reader is referred to the Web version of this article.)

cadherin) and transcription factors (SNAIL1/2 and TWIST) [39]. In this study, VCC1 showed increased expression of vimentin and Twist-1 and decreased E-cadherin levels, indicating an EMT-like phenotype, however retaining cytokeratin expression. Combined, these results suggest an intermediate EMT-like phenotype of VCC1 and supports the notion that VLS-VSCC tumors have high metastatic potential [6].

3D OTC provides a reproducible and high-throughput assay mimicking the native epithelium in stratification, organization and cell-cell interactions [38,40]. 3D OT models have a varied number of applications including drug screening prior to *in vivo* studies and deciphering the role of tumor stroma [13,38,41]. VCC1 showed little to no invasion into the underlying collagen matrix in the absence of fibroblasts in 3D OTC. In contrast, VCC1 invaded the collagen matrix irrespective of the presence of normal or cancer-associated fibroblasts. These results are in line with the study of Gaggioli et al. [42] and studies done in our lab [13,41] where the importance of fibroblasts for invasion of SCC cells has been well documented.

In spite of the immortal growth behavior of VCC1 *in vitro*, VCC1 alone failed to form continuously growing tumors in mice. This corroborates with previous findings using mice xenografts with UMSCV1A, where this cell line did not form invasive tumors and failed to develop continuously growing tumors [14]. However, VCC1 with VCAF1 formed continuously growing tumors suggesting that cancer-associated fibroblasts can enhance the tumor-forming capability of VCC1 and support their survival. In addition, the histology and local invasion profile was similar between the original tumor and xenografts with VCAFs but not with VCC1 alone. Taken together, both in 3D OTC and xenografts models points to the key role of stromal fibroblasts in carcinogenesis of VLS-VSCC. Although, the investigation of tumor-stroma cross talk is beyond the scope this study, we postulate that our novel cell line VCC1, along with 3D OTC and xenograft models established here will serve as the basis for further studies. Moreover, these 3D models could serve as preclinical tools to determine changes associated with the extracellular matrix in squamous cell carcinoma development in the supra-adjacent epithelium. This could enhance our understanding of the tumor-stroma cross talk in inflammatory scarring skin diseases such as VLS. In a longer perspective, this could be beneficial in developing biomarkers, which can stratify patients with VLS having a higher likelihood of evolving into VSCC.

In conclusion, we herein report the establishment of a novel cell line, VCC1. It showed characteristic epithelial morphology with increased stemness as well as migratory and invasive phenotypes than already established VSCC cell lines. In addition, these cells are tumorigenic *in vivo* only when injected together with cancer-associated fibroblasts suggesting a crucial role of fibroblasts in VLS-related oncogenesis. Our findings suggest that this cell line could be beneficial in

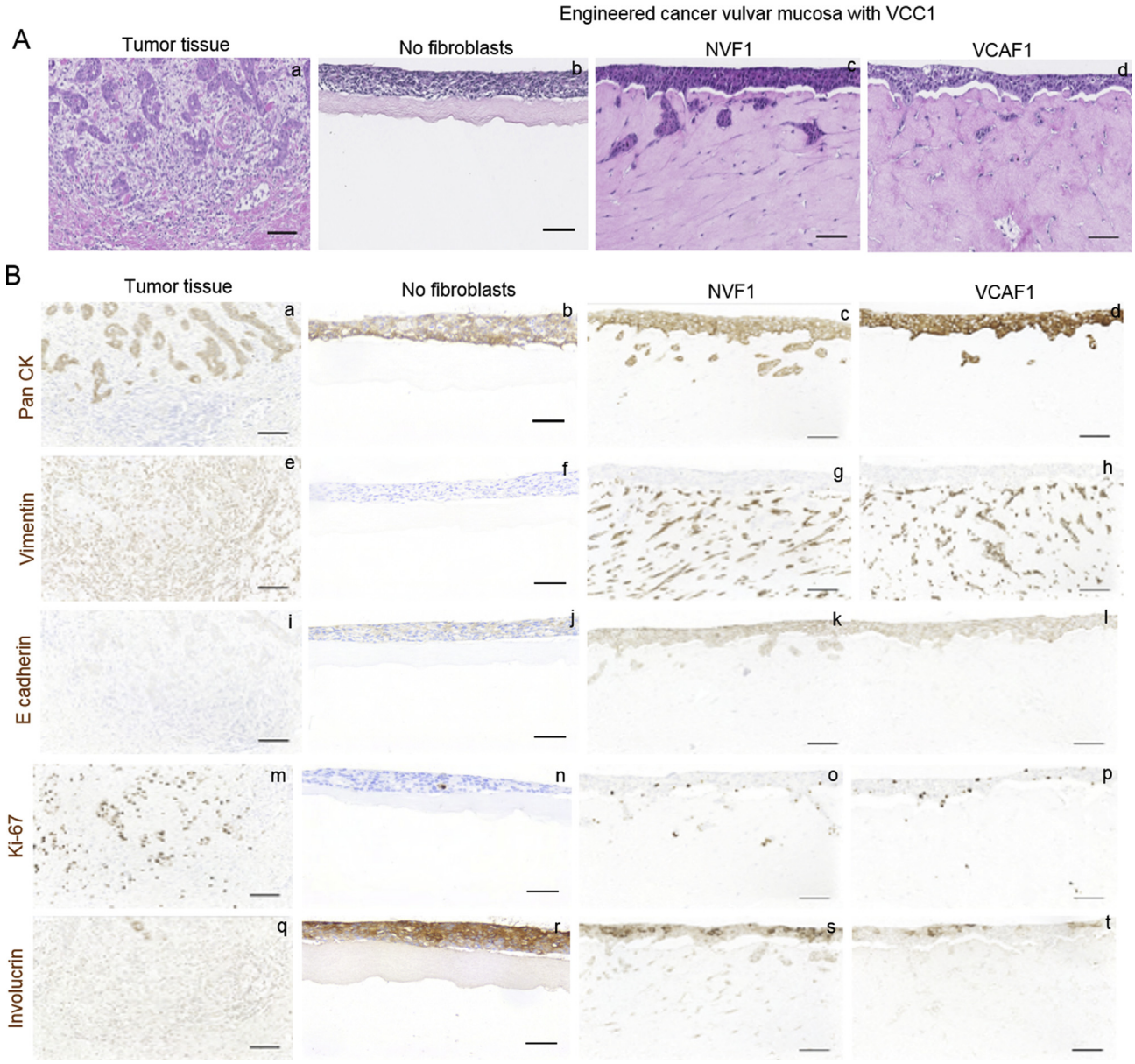

Fig. 4. Histology and immunohistochemistry of engineered vulvar cancer mucosa in comparison to native tissue. A) Representative images of H&E stained vulvar cancer mucosa 3D OTC's grown without fibroblasts (b), with normal vulvar fibroblasts (c, NVF1) and cancer-associated fibroblasts (d, VCAF1) in comparison to tumor tissue (a). B) Immunohistochemistry using antibodies against Pan-cytokeratin (a, b, c, d) (Pan-CK) was used to confirm the epithelial nature of cells in 3D OTCs. Antibodies against vimentin (e, f, g, h) and E-cadherin (i, j, k, l) were used to study epithelial-mesenchymal transition and Ki-67 (m, n, o, p) and involucrin (q, r, s, t) were used as markers of proliferation and differentiation respectively in native vulvar tumor tissue and 3D OTC grown with and without fibroblasts. Scale bar-100 μm.

elucidating the carcinogenesis of vulva cancer associated with lichen sclerosus and the tumor-stroma cross talk.

Declaration of competing interests

None.

Acknowledgements

The authors thank Rasmus Kopperud Riis for his assistance in STR profiling. The authors also acknowledge the use of Flow Cytometry Core Facility at the Department of Clinical Science, University of Bergen. Funding support: This work was supported by the Norwegian Centre of Excellence grant (ID 223250), the Western Norway Regional Health Authority (Helse Vest project nr. 912260) and the Norwegian Centre for International Cooperation in Education (project nr. CPEA-LT-2016/10106).

Appendix A. Supplementary data

Supplementary data to this article can be found online at https://doi.org/10.1016/j.yexcr.2019.111684.

Transparency document

Transparency document related to this article can be found online at https://doi.org/10.1016/j.yexcr.2019.111684.

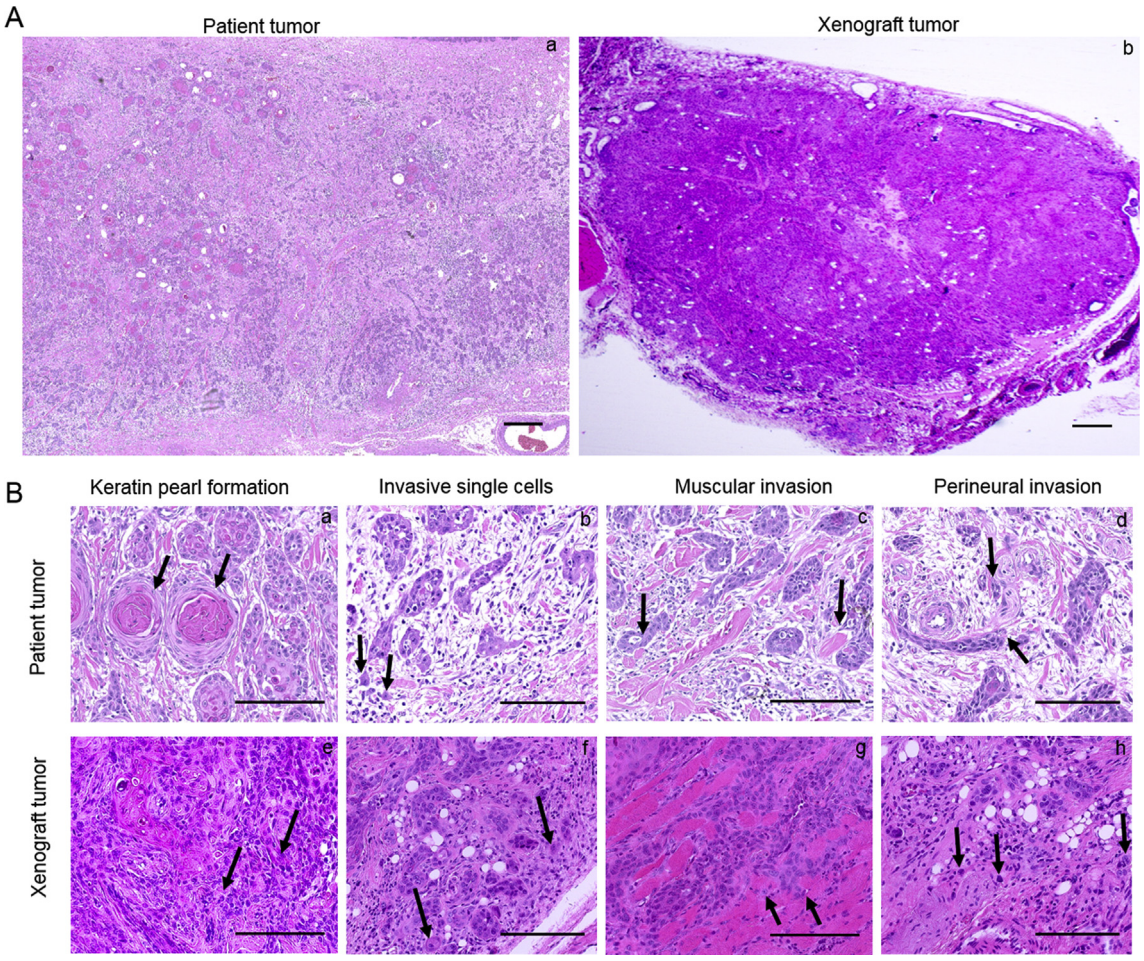

Fig. 5. H&E staining of patient tumor and mice xenografts showing similar histological features. A) Overview of patient tumor (a) and whole tumor mice xenograft (b) developed in NOD/SCID IlŸ2R deficient mice. Scale bar-1mm. B) Comparison of histological features such as keratin pearl formation (a, e), invasive single cell and small islands at the tumor front (b, f), muscular invasion (c, g) and perineural invasion (d, h) (all marked with black arrows) in between patient tumor and xenografts. Scale bar-100 μm.

References

[1] C.J. Meltzer-Gunnes, M.C. Smastuen, G.B. Kristensen, C.G. Trope, A.K. Lie, I. Vistad, Vulvar carcinoma in Norway: a 50-year perspective on trends in incidence, treatment and survival, Gynecol. Oncol. 145 (2017) 543–548.

[2] L.N. Hoang, K.J. Park, R.A. Soslow, R. Murali, Squamous precursor lesions of the vulva: current classification and diagnostic challenges, Pathology 48 (2016) 291–302.

[3] M.C. Bleeker, P.J. Visser, L.I.H. Overbeek, M. van Beurden, J. Berkhof, Lichen Sclerosus: Incidence and Risk of Vulvar Squamous Cell Carcinoma, Cancer Epidemiology Biomarkers &amp, Prevention, 2016 cebp.0019.2016.

[4] A. Terlou, L.J. Blok, T.J. Helmerhorst, M. van Beurden, Premalignant epithelial disorders of the vulva: squamous vulvar intraepithelial neoplasia, vulvar Paget's disease and melanoma in situ, Acta Obstet. Gynecol. Scand. 89 (2010) 741–748.

[5] M.L. Harmon, Premalignant and malignant squamous lesions of the vulva, Diagn. Histopathol. 16 (2010) 500–508.

[6] L.J. Rogers, M.A. Cuello, Cancer of the vulva, Int. J. Gynecol. Obstet. 143 (2018) 4–13.

[7] P.A. Cohen, L. Anderson, L. Eva, J. Scurry, Clinical and molecular classification of vulvar squamous pre-cancers, Int. J. Gynecol. Cancer 29 (2019) 821–828.

[8] P.A. Cohen, L. Anderson, L. Eva, J. Scurry, Clinical and molecular classification of vulvar squamous pre-cancers, Int. J. Gynecol. Cancer 29 (2019) 821–828.

[9] P.A. Nair, Vulvar lichen sclerosus et atrophicus, J. Mid Life Health 8 (2017) 55–62.

[10] S.M. Neill, F.M. Tatnall, N.H. Cox, Guidelines for the management of lichen sclerosus, Br. J. Dermatol. 147 (2002) 640–649.

[11] L. Micheletti, M. Preti, G. Radici, S. Boveri, O. Di Pumpo, S.S. Privitera, B. Ghiringhello, C. Benedetto, Vulvar lichen sclerosus and neoplastic transformation: a retrospective study of 976 cases, J. Low. Genit. Tract Dis. 20 (2016) 180–183.

[12] P. Carli, A. De Magnis, F. Mannone, E. Botti, G. Taddei, A. Cattaneo, Vulvar carcinoma associated with lichen sclerosus. Experience at the Florence, Italy, Vulvar Clinic, J. Reprod. Med. 48 (2003) 313–318.

[13] D.E. Costea, K. Kulasekara, E. Neppelberg, A.C. Johannessen, O.K. Vintermyr, Species-specific fibroblasts required for triggering invasiveness of partially transformed oral keratinocytes, Am. J. Pathol. 168 (2006) 1889–1897.

[14] M. Raitanen, M.J. Worsham, T. Lakkala, T.E. Carey, D.L. Van Dyke, R. Grenman, P. Klemi, V. Rantanen, J. Isola, S. Grenman, Characterization of 10 vulvar carcinoma cell lines by karyotyping, comparative genomic hybridization and flow cytometry, Gynecol. Oncol. 93 (2004) 155–163.

[15] P.B.G.d. Silva, C.O. Rodini, C. Kaid, A.M. Nakahata, M.C.L. Pereira, H. Matushita, S.S.d. Costa, O.K. Okamoto, Establishment of a novel human medulloblastoma cell line characterized by highly aggressive stem-like cells, Cytotechnology 68 (2016) 1545–1560.

[16] X. Liang, T.A.-H. Osman, D. Sapkota, E. Neppelberg, S. Lybak, P.G. Liavaag, A.C. Johannessen, H.K. Jacobsen, P.Ø. Enger, D.E. Costea, J. Wang, Rapid adherence to collagen IV enriches for tumour initiating cells in oral cancer, Eur. J. Cancer 50 (2014) 3262–3270.

[17] H. Parajuli, M.-T. Teh, S. Abrahamsen, I. Christoffersen, E. Neppelberg, S. Lybak, T. Osman, A.C. Johannessen, D. Gullberg, K. Skarstein, D.E. Costea, Integrin α11 is overexpressed by tumour stroma of head and neck squamous cell carcinoma and correlates positively with alpha smooth muscle actin expression, J. Oral Pathol. Med. Off. Publ. Int. Assoc. Oral Pathol. Am. Acad. Oral Pathol. 46 (2017) 267–275.

[18] S. Teppo, E. Sundquist, M. Vered, H. Holappa, J. Parkkisenniemi, T. Rinaldi, P. Lehenkari, R. Grenman, D. Dayan, J. Risteli, T. Salo, P. Nyberg, The hypoxic tumor microenvironment regulates invasion of aggressive oral carcinoma cells, Exp. Cell Res. 319 (2013) 376–389.

[19] L.D. Shultz, B.L. Lyons, L.M. Burzenski, B. Gott, X. Chen, S. Chaleff, M. Kotb, S.D. Gillies, M. King, J. Mangada, D.L. Greiner, R. Handgretinger, Human lymphoid and myeloid cell development in NOD/LtSz-scid IL2R gamma null mice engrafted with mobilized human hemopoietic stem cells, J. Immunol. 174 (2005) 6477–6489 Baltimore, Md. : 1950.

[20] A.A. Nery, I.C. Nascimento, T. Glaser, V. Bassaneze, J.E. Krieger, H. Ulrich, Human mesenchymal stem cells: from immunophenotyping by flow cytometry to clinical applications, Cytometry Part A 83A (2013) 48–61.

[21] N. Johansson, M. Vaalamo, S. Grenman, S. Hietanen, P. Klemi, U. Saarialho-Kere, V.M. Kahari, Collagenase-3 (MMP-13) is expressed by tumor cells in invasive vulvar squamous cell carcinomas, Am. J. Pathol. 154 (1999) 469–480.

[22] A.S. Cheng, A.N. Karnezis, S. Jordan, N. Singh, J.N. McAlpine, C.B. Gilks, p16 immunostaining allows for accurate subclassification of vulvar squamous cell carcinoma into HPV-associated and HPV-independent cases, Int. J. Gynecol. Pathol. 35 (2016) 385–393.
[23] T. Buchanan, D. Mutch, Squamous cell carcinoma of the vulva: a review of present management and future considerations, Expert Rev. Anticancer Ther. 19 (2019) 43–50.
[24] A.A. Clancy, J.N. Spaans, J.I. Weberpals, The forgotten woman's cancer: vulvar squamous cell carcinoma (VSCC) and a targeted approach to therapy, Ann. Oncol. 27 (2016) 1696–1705.
[25] L.S. Nooij, F.A.M. Brand, K.N. Gaarenstroom, C.L. Creutzberg, J.A. de Hullu, M.I.E. van Poelgeest, Risk factors and treatment for recurrent vulvar squamous cell carcinoma, Crit. Rev. Oncol.-Hematol. 106 (2016) 1–13.
[26] D.N. Slater, B.E. Wagner, Early vulvar lichen sclerosus: a histopathological challenge, Histopathology 50 (2007) 388–389 author reply 389-391.
[27] S. Louzada, F. Adega, R. Chaves, Defining the sister rat mammary tumor cell lines HH-16 cl.2/1 and HH-16.cl.4 as an in vitro cell model for Erbb2, PLoS One 7 (2012) e29923.
[28] W.C. van Staveren, D.Y. Solis, A. Hebrant, V. Detours, J.E. Dumont, C. Maenhaut, Human cancer cell lines: experimental models for cancer cells in situ? For cancer stem cells? Biochim. Biophys. Acta 1795 (2009) 92–103.
[29] J. Jung, Human tumor xenograft models for preclinical assessment of anticancer drug development, Toxicol. Res. 30 (2014) 1–5.
[30] T. Vargo-Gogola, J.M. Rosen, Modelling breast cancer: one size does not fit all, Nat. Rev. Cancer 7 (2007) 659–672.
[31] M. Singh, L. Johnson, Using genetically engineered mouse models of cancer to aid drug development: an industry perspective, Clin. Cancer Res. 12 (2006) 5312–5328.
[32] P. Zhang, B.D. Lehmann, Y. Shyr, Y. Guo, The utilization of formalin fixed-paraffin-embedded specimens in high throughput genomic studies, Int. J. Genom. (2017) 9 2017.
[33] V. Musella, M. Callari, E. Di Buduo, M. Scuro, M. Dugo, P. Miodini, G. Bianchini, B. Paolini, L. Gianni, M.G. Daidone, V. Cappelletti, Use of formalin-fixed paraffin-embedded samples for gene expression studies in breast cancer patients, PLoS One 10 (2015) e0123194e0123194.
[34] N. Niu, L. Wang, In vitro human cell line models to predict clinical response to anticancer drugs, Pharmacogenomics 16 (2015) 273–285.
[35] K. Kiguchi, I. Ishiwata, C. Ishiwata, M. Iwata, B. Ishizuka, H. Yoshikawa, T. Tachibana, H. Hashimoto, H. Ishikawa, Establishment and characterization of two squamous cell carcinoma cell lines (HYVC and HMVC) derived from vulva, Hum. Cell 15 (2002) 207–214.
[36] S.M. Rothenberg, G. Mohapatra, M.N. Rivera, D. Winokur, P. Greninger, M. Nitta, P.M. Sadow, G. Sooriyakumar, B.W. Brannigan, M.J. Ulman, R.M. Perera, R. Wang, A. Tam, X.-J. Ma, M. Erlander, D.C. Sgroi, J.W. Rocco, M.W. Lingen, E.E.W. Cohen, D.N. Louis, J. Settleman, D.A. Haber, A genome-wide screen for microdeletions reveals disruption of polarity complex genes in diverse human cancers, Cancer Res. 70 (2010) 2158–2164.
[37] M.V. Verga Falzacappa, C. Ronchini, L.B. Reavie, P.G. Pelicci, Regulation of self-renewal in normal and cancer stem cells, FEBS J. 279 (2012) 3559–3572.
[38] I.C. Mackenzie, Growth of malignant oral epithelial stem cells after seeding into organotypical cultures of normal mucosa, J. Oral Pathol. Med. 33 (2004) 71–78.
[39] S. Lamouille, J. Xu, R. Derynck, Molecular mechanisms of epithelial-mesenchymal transition, Nat. Rev. Mol. Cell Biol. 15 (2014) 178–196.
[40] A. Hansson, B.K. Bloor, Y. Haig, P.R. Morgan, J. Ekstrand, R.C. Grafström, Expression of keratins in normal, immortalized and malignant oral epithelia in organotypic culture, Oral Oncol. 37 (2001) 419–430.
[41] D.E. Costea, A. Hills, A.H. Osman, J. Thurlow, G. Kalna, X. Huang, C. Pena Murillo, H. Parajuli, S. Suliman, K.K. Kulasekara, A.C. Johannessen, M. Partridge, Identification of two distinct carcinoma-associated fibroblast subtypes with differential tumor-promoting abilities in oral squamous cell carcinoma, Cancer Res. 73 (2013) 3888–3901.
[42] C. Gaggioli, S. Hooper, C. Hidalgo-Carcedo, R. Grosse, J.F. Marshall, K. Harrington, E. Sahai, Fibroblast-led collective invasion of carcinoma cells with differing roles for RhoGTPases in leading and following cells, Nat. Cell Biol. 9 (2007) 1392.